Available online at www.sciencedirect.com

ScienceDirect

Physics Procedia 56 (2014) 269 – 275

Physics Procedia

8th International Conference on Photonic Technologies LANE 2014

Laser cladding of Ni-WC layers with graded WC content

J.M. Amado[a], J. Montero[a], M.J. Tobar[a,]*, A. Yáñez[a]

[a]*Universidade da Coruña. Escola Politécnica superior. 15403 Ferrol, Spain.*

Abstract

Coating techniques using powder as added material can be adapted for the manufacture of composition gradients if a mixing unit is included in the powder feed system. As for the laser cladding technology, FGM can be obtained if mixing parameters are changed along the process. This work deals with the development of NiCrBSi layers with WC graded composition. The purpose is to obtain longitudinal compositional gradients within distances of millimeters along a laser scan. To accomplish this task, the capabilities and time delays in the feeding system are identified and analyzed. Preliminar tests on single cladding beads show results in reasonable agreement with expectations.

Peer-review under responsibility of the Bayerisches Laserzentrum GmbH

Keywords: laser cladding; tungsten carbide; FGM

1. Introduction

In recent years, as the environments in which materials are used become more demanding, there are frequently cases in which the conventional homogeneous materials cannot withstand severe working conditions. To meet the increasing requirement for industrial materials, studies have been conducted to design inhomogeneous composites, such as coated and joined materials. However, these materials possess sharp boundaries, the existence of which often results in various undesirable behavior caused by the discontinuities in the physical and chemical characteristics at the boundary

In a general definition, an FGM is a composite consisting of two or more phases, structures or textures, which vary gradually in a certain direction. In general, the applications of the FGM concept are based on combining two or

* Corresponding author. Tel.: +34-981-337400Ext3357; fax: +34-981-337416 .
E-mail address: maria.jose.tobar@udc.e

Peer-review under responsibility of the Bayerisches Laserzentrum GmbH
doi:10.1016/j.phpro.2014.08.171

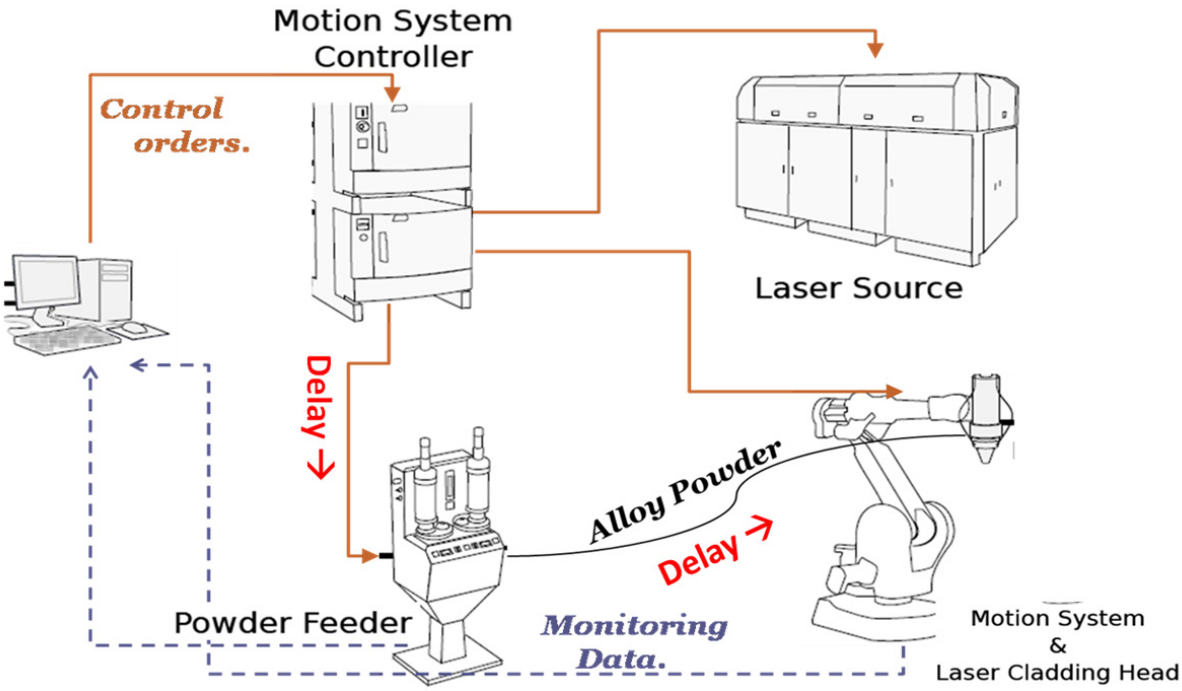

Fig. 1. Laser Cladding system layout.

more incompatible functions into a given material [W. M. Steen(2006), K. Shin et al (2003), I. Yadroitsev et al. (2007)].

Coating techniques using powder as added material can be adapted for the manufacture of composition gradients if a mixing unit is included in the powder feed system. The powder feed is the basis of laser cladding technology for the production of layers with composition closer to the fed material. FGM can be obtained if mixing parameters are changed along the process

The development of NiCr-WC composited coatings have been the subject of previous works done by the authors. In [J.M. Amado et al(2011)] NiCr-WC composited coatings, with 60%wt. carbide concentration were deposited by laser cladding. Three commercial premixed materials were used which differed in the chromium concentration of the NiCrBSi metal matrix. In all cases preheating procedures were needed to avoid the cracking susceptibility of the deposited coatings. In [J.M. Amado et al(2012)], WC graded coatings made up of two superimposed layers with increasing WC concentration were developed. It was proved that a 15%wt. WC concentration on the intermediate layer allowed the deposition of a subsequent 60%wt. carbide concentration layer without preheating needs. This implies a significant advantage for the hardfacing process, simplifying the procedure and therefore increasing productivity. This also means that the production of softer boundaries, *i.e.* smaller difference in the concentration of the reinforcement phase among consecutive layers, favors the obtention of crack free coats with high ceramic content.

The development of superimposed cladding layers with increasing WC content has no other specific technical difficulties than those of standard laser cladding process. The mixing ratios of powders employed have to be set at the beginning of the layer deposition and changed as desired on successive overlays, but remain constant along the deposition of each clad bead. However, if the objective is to obtain a graded structure along the scanning direction, this is, a varying WC percentage along an individual laser scan, additional processing strategies are required. In this case, mixing ratios have to be changed online during material deposition and a careful calibration of the system delays and powder feeding capabilities has to be performed to ensure the required composition is obtained at any specified location of the cladding bead.

In this work several steps are given to properly characterize the system and enable a successful building of functionally graded parts. Given a certain path planning, including the relative concentration of the reinforcement phase, it will be established whether or not this graded is reachable, what changes on the concentration are possible and how to modify the process parameters to achieve the designed concentration

2. Experimental

Fig. 1 shows schematically the main components of the laser cladding system. It is composed of a continuous wave diode pumped Nd:YAG laser (Rofin DY022) with a maximum power of 2200 W. Laser is sent through a fiber to the YC50 Precitec cladding head installed in a ABB IRB2400 six axis robot arm. Powder feeding is made with a Sulzer-Metco Twin 10C unit, which counts with two hoppers allowing for online alloy powder mixing. A linux based application developed by the authors controls and monitors all the steps of the process. Programming commands are transmitted via ftp and loaded into the ABB motion controller. Once loaded, the controller takes upon the movement of the robot according to the programmed speed and trajectory. It also sends the required voltage signals for switching on the laser and the powder feeder and sets the required laser power and powder flow levels during the process. Return monitoring signals from laser cladding head and powder feeder are directly transmitted to the PC application for process supervision. A standard CCD camera connected to the PC was also used in the study to determine the powder feeding delay.

As for the cladding materials, the NiCr-WC layers were produced from a mixture of NiCrBSi (Deloro 30) and tungsten carbide WC (Woka 3303) alloys.. The nominal hardness of the metallic matrix alloy is 30 HRC. WC powder is of the cemented carbide type. The NiCr and WC were separately stored in each of the two powder feeding hoppers. Both hoppers were calibrated independently and the mixing of the two materials was performed in flight. The mixing parameters were automatically changed by the robot controller. Cladding was performed on 10 mm thick probes of A304 steel. Laser beam was defocused to a diameter of 3mm on the working surface.

3. Results and Discussion

3.1. Analysis of powder feeding system.

As noted in the description of the experimental set-up, the robot controller sends startup signals for the laser power, robot and powder feeder. Once the cladding head is conveniently positioned on the working plane, upon controller orders the required laser power level and scan speed are readily available. In other words, time delays between controller settings and laser power and robot movement are not significant in our process. However, a waiting time in the order of seconds is needed to achieve the desired value of the powder flow projected through the cladding nozzle. This delay is caused in first place by the dynamics or the rotating disc of the powder feeder and in second place by the travelling path along feeding tubes from the feeder to the nozzle.

The powder feed rate is proportional to the rotational speed of the rotating disc. Following calibration, the desired powder flow rate is set as a percentage of the maximum speed value of the disc. Fig. 2.a) shows the calibration results for the NiCrBSi and WC powders, in their respective hoopers. Monitoring data of the powder feeder upon a 20% setting (20% of maximum r.p.m) is shown in Fig. 2.b). The rotation speed increases linearly and arrives to the preset value after 1-2 seconds. Obviously, the slope of the line represents the acceleration of the rotating disc. The behavior of the two individual hoppers (shown in red and blue respectively) is similar although some minor difference exists due to their individual hardware configurations in the feeder.

Threfore, calibration defines a linear relation between the powder flow (in grams per second) of the WC powder g_{WC} and the rotational speed of the feeder disc v_d (in % r.p.m) as:

$$g_{WC} = a \cdot v_d + b \tag{1}$$

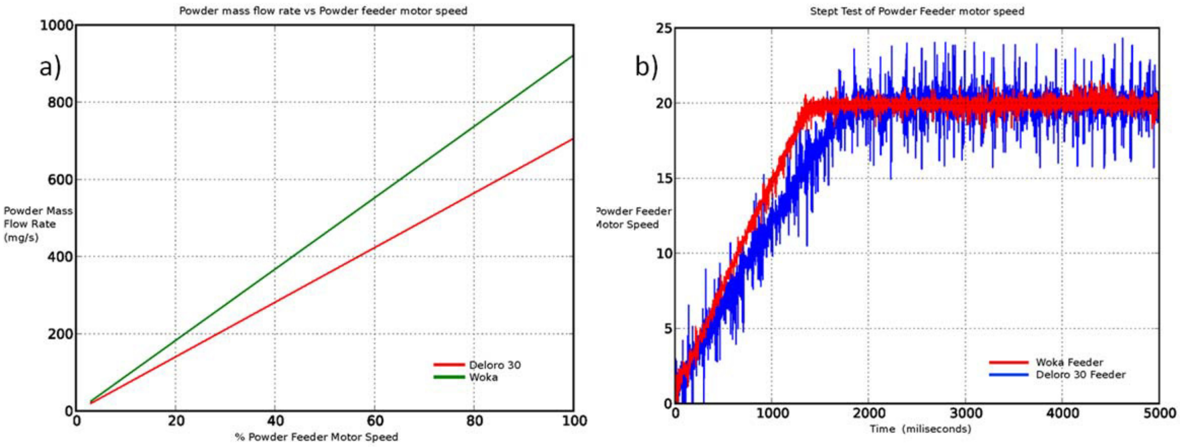

Fig. 2. (a) Feeder calibration of NiCr and WC powders; (b) Time evolution of the hoppers rotating discs speed following a 20% r.p.m. setting.

If m represents the acceleration of the rotating disc, i.e., the slope of the line shown in Fig 2., the time t_1 needed to achieve a feed rate g_{WC} at the exit of the feeder is:

$$t_1 = \frac{v_d}{m} = \frac{g_{WC} - b}{a \cdot m} \tag{2}$$

In order to measure the delay time given by the path length between the powder feeder and the cladding head, a CCD camera was used to record the powder stream through the nozzle. In Fig. 3 (a) shows an example of an image frame where the low part of the nozzle is visible. The powder stream illuminated by an external source can also be appreciated. Binarization of this image leads to the picture shown in Fig. 3.b). By counting the bright pixels on the picture, an integrated area is obtained which should be proportional to the powder flow rate through the nozzle.

A series of test were performed by setting the value of the powder rate in the feeders according to triangular pulse shapes, as shown in red Fig. 3 c) and d). They correspond to the hoppers where the WC and the NiCr alloy are respectively stored. The voltage signal represents one tenth of the rotating disc speed v_d (i.e. 2V means 20% r.p.m). The corresponding image frame analysis of the CCD recordings at the exit of the nozzle is shown in the same Fig.s in blue. The startup signals for powder feeder and CCD are synchronized. It is clear that the recorded image area reproduces the powder flow settings except for a time shift determined by the travel path of the powder along the feeding lines. This time shift t_2 has been measured as 1.35 s in the Woka hopper and 1.70 in the Deloro 30 one.

Thus, recalling Eq (2), the total powder delay time t_p is:

$$t_p = t_1 + t_2 = \frac{g_{WC} - b}{a \cdot m} + t_2 \tag{3}$$

Therefore, if a certain g_{WC} value is to be projected on the working area at a particular time the powder setting should be communicated with t_p seconds in advance. Furthermore, if the WC rate is to be changed by Δg_{WC} within a length L along laser scan, it would require a time Δt_p given by:

$$\Delta t_p = \frac{\Delta g_{WC}}{a \cdot m} \tag{4}$$

However, and depending on laser scan speed v_L, Δt_p may be larger than the time taken by the laser to travel the L distance. A limit is thus imposed on the WC rate change achievable per unit length and given by:

$$\Delta t_p = \frac{\Delta g_{WC}}{a \cdot m} \le \frac{L}{v_L} \quad \Rightarrow \frac{\Delta g_{WC}}{L} \le \frac{a \cdot m}{v_L} \tag{5}$$

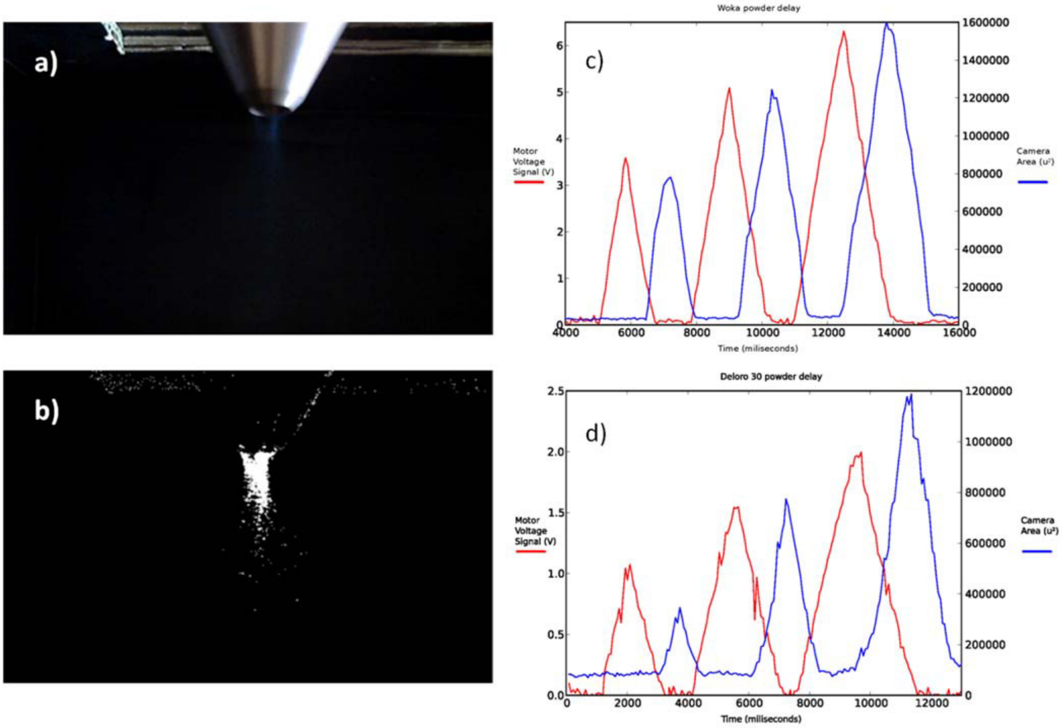

Fig. 3. Powder stream through cladding nozzle before (a) and after (b) binarization of the image; (c), (d) In red, powder flow input signal in feeder hoppers. In blue, corresponding powder flow at the exit of the nozzle measured as the bright area in binarized images.

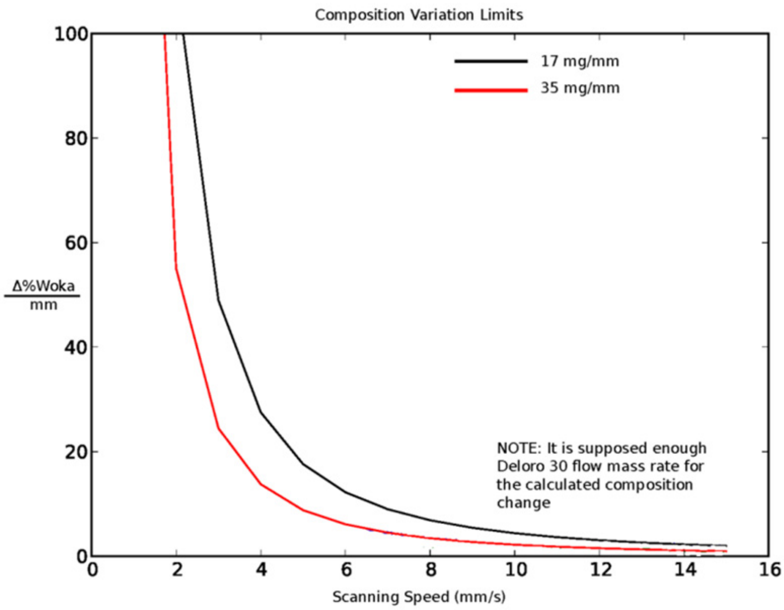

Fig. 4. Maximum values allowed for WC wt% variation per mm length as function of scanning speed.

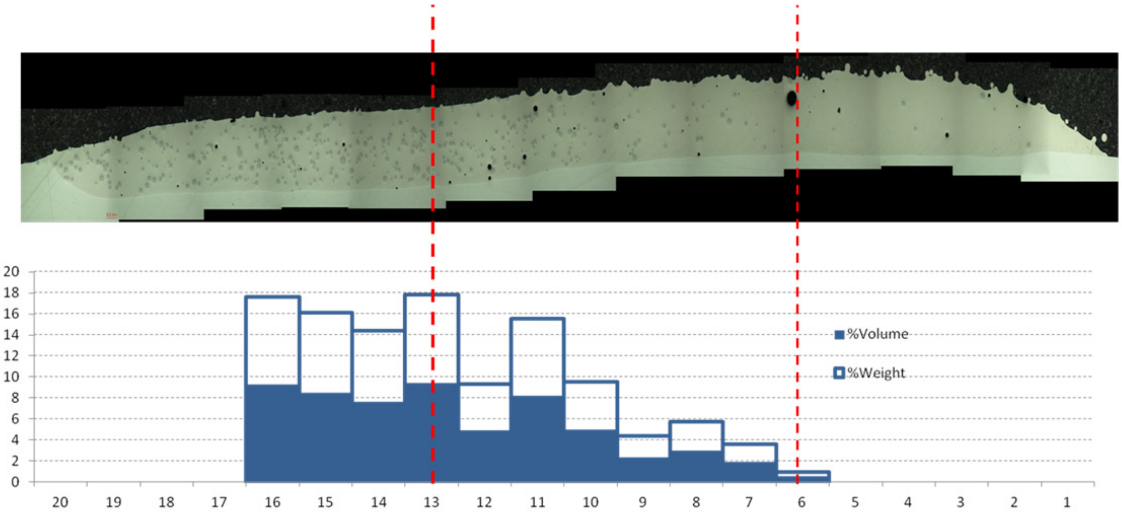

Fig. 5. Longitudinal section cut of cladding bead with designed WC grading in the length delimited by the dash, red lines. Volume (solid bars) and Weight (open bars) WC ratios obtained per mm length by stereology-image analysis.

Denoting as ω_{WC} the weight fraction of WC in the powder, $\omega_{WC}= g_{WC}/g$, with $g= g_{WC}+g_{D30}$ being total powder rate, equation (5) can be rewritten in terms of WC wt% ratio change per unit distance as:

$$\frac{\Delta\omega_{WC}}{L} \leq \frac{a \cdot m}{g \cdot v_L} \quad (6)$$

Expressing Eq. (6) not in terms of feed rate g (= grams per seconds) but of powder feed per mm along laser scan $f=g/v_L$ (grams per mm):

$$\frac{\Delta\omega_{WC}}{L} \leq \frac{a \cdot m}{f \cdot v_L^2} \quad (7)$$

Fig. 4. shows the upper limit for WC wt.% variation per mm in the powder mixture calculated according to Eq (7). It is been calculated for f= 17 mg/mm and f= 35 mg/mm. It is seen that low scan speeds admits a significant change of WC ratio along processed clad beads. On increasing scanning speeds, the allowed change is significantly reduced. This reduction is larger on feeding at bigger powder weights per mm. Finally, it should also be noted that all the above discussion and the results shown on the Fig. obviate the limits imposed by the hardware capabilities of the power feeder: neither g_{WC} nor g_{D30} can be larger than the value corresponding to the maximum rotation speed of the disc v_d= 100% rpm.

3.2. WC grading results on cladding samples

The performance of the analyzed system in WC grading deposition was tested on single laser scans. Fig. 5 illustrates the results obtained. 1450 W laser power were applied at 5 mm/s scan speed. The test was designed so as to deposit a cladding bead with 20 mm length. The composition should start with 100%wt. NiCr and continue during the first 7.5 mm. At this point, a WC %wt ratio was to be linearly varied from 0% to 20% along 7 mm and kept constant (20%) till the end of the scan (last 5.5 mm). Powder feeder settings in order to start WC deposition at 7.5 mm were done observing delay times as described in Eq (3). The WC grading along the next 7 mm was performed by dividing the time needed to travel the 7 mm length (~ 1.4 s) into intervals of 0.1 s. At each interval powder settings were changed so as to obtain the prescribed increase $\Delta\omega_{WC}$ =2.85 % per mm (20%/7mm).

A longitudinal sectional cut of the deposited material, shown in Fig 5, was inspected and analyzed by image analysis. The WC ratio along the clad bead was calculated based on stereology analysis [G. F. Vander Voort(2007)]. Within this frame, according to Delesse Principle, the area fraction obtained on bidimensional sections is an estimate of the volume fraction. Therefore, by selecting the pixel area corresponding to the carbides and dividing it by the total pixel area in the image, an estimate of the volume ratio of the carbides at the position taken by the image is obtained.

In the low part of Fig. 5, a bar plot (solid blue) is shown representing the mean WC volume fraction measured by millimeter along the section. The green, red lines delimitate the interval with graded composition. As expected , the WC ratio increase and stabilizes at the prescribed positions. Conversion from volume to weight ratios gives values close to expectation as well.

4. Conclusions

Characteristics and capabilities of the powder feeding in the laser cladding system have been analyzed. Time delays between the setting of powder flow rate values by the process control and the corresponding flow through the cladding nozzle have be identified and quantified. These delays (estimated in a few seconds) are related to the dynamics of rotating disc in the feeder hoppers and the traveling time along feeding tubes to the cladding head. They defined the maximum WC %wt. ratio change feasible per unit length. Tests were designed, accounting for feeding system analysis results, to obtain WC %wt gradings of about 3% per millimeter. Results con cladded samples show a reasonable agreement with expectations.

References

Steen, W.M. (2006): Laser Material Processing, 3rd ed. (Springer-Verlag, London-Berlin-Heidelberg.

K. Shin et al. (2003) A method for the design and fabrication of heterogeneous objects. Materials and Design 24, 339-353

I. Yadroitsev et al. (2007) Application of laser assisted technologies for fabrication of functionally graded coatings and objects for the International Thermonuclear Experimental Reactor components. Journal of Nuclear Materials 362 189-196..

J.M. Amado et al. (2011) Crack Free Tungsten Carbide Reinforced Ni(Cr) Layers obtained by Laser Cladding. Physics Procedia 12, 338-344.

J. M. Amado et al. (2012) Ni-based metal matrix composite functionally graded coatings. Physics Procedia, 39, 362-367

G. F. Vander Voort (2007) Metallography Principles and Practice. ASM International.